

**Radiative corrections to dilepton
production at LHC:
the Drell–Yan process
vs
the Photon Fusion mechanism**

V. A. Zykunov (JINR, GSU)

Dubna, 30 May, 2024

Introduction

Despite the fact that the Standard Model (SM) keeps for oneself the status of consistent and experimentally confirmed theory, the search of New Physics (NP) manifestations is continued:

- ★ **the supersymmetry,**
- ★ **M-theory,**
- ★ **DM-particles,**
- ★ **axions,**
- ★ **feebly interacting particles,**
- ★ **extra spatial dimensions,**
- ★ **extra neutral gauge bosons, etc.**

One of powerful tool in the modern experiments at LHC is the investigation of **Drell–Yan dilepton production**

$$pp \rightarrow \gamma, Z \rightarrow l^+ l^- X \quad (1)$$

at **large invariant mass** of lepton pair: $M \geq 1$ TeV.

Drell-Yan process (1970, BNL)

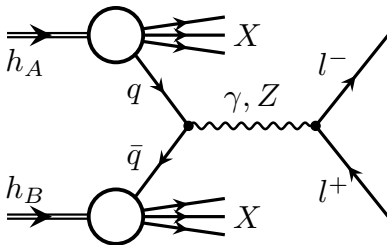


Figure 1: Drell-Yan process with neutral current

- ★ \sqrt{S} is total energy in c.m.s. of hadrons
- ★ M is dilepton l^+l^- invariant mass ($l = e, \mu$)
- ★ y is dilepton rapidity

- ★ The measured Drell–Yan cross sections and forward-backward asymmetries are consistent with the SM predictions at

$$\sqrt{S} = 7\text{--}8 \text{ TeV} (19.7 \text{ fb}^{-1}) \text{ for } M \leq 2 \text{ TeV},$$

$$\sqrt{S} = 13 \text{ TeV} (85 \text{ fb}^{-1}) \text{ for } M \leq 3 \text{ TeV}$$

- ★ differential cross section $\frac{d\sigma}{dM}$,
 - ★ double-differential cross section $\frac{d^2\sigma}{dMdy}$,
 - ★ forward-backward asymmetry A_{FB} .
- ★ NNLO RCs are taken into account by using of **FEWZ**,
 - ★ NNLO PDFs are **CT10 NNLO** and **NNPDF2.1**.

Some modern codes for NLO and NNLO RC for DY process at hadronic colliders (in the ABC order)

- ★ DYNNLO (S. Catani, L. Cieri, G. Ferrera et al.)
- ★ FEWZ (R. Gavin, Y. Li, F. Petriello, S. Quackenbush)
- ★ HORACE (C. Carloni Calame, G. Montagna, et al.)
- ★ MC@NLO (S. Frixione, F. Stoeckli, P. Torrielli et al.)
- ★ PHOTOS (N. Davidson, T. Przedzinski, Z. Was et al.)
- ★ POWHEG (L. Barze, G. Montagna, P. Nason et al.)
- ★ RADY (S. Dittmaier, A. Huss, C. Schwinn et al.)
- ★ READY (V. Zykunov, RDMS CMS)
- ★ SANC (Dubna: A. Andonov, A. Arbuzov, D. Bardin et al.)
- ★ WINHAC (W. Placzek, S. Jadach, M. W. Krasny et al.)
- ★ WZGRAD (U. Baur, W. Hollik, D. Wackerroth et al.)

Code READY and a set of prescriptions

In the following the scale of radiative corrections and their effect on the observables of Drell–Yan processes will be discussed using FORTRAN program **READY**: (**R**adiative corr**E**ctions to **L**arge invariant mass **D**rell–**Y**an process).

We used the following set of prescriptions:

- ★ standard PDG set of SM input electroweak parameters,
- ★ “effective” quark masses ($\Delta\alpha_{had}^{(5)}(m_Z^2) = 0.0276$),
- ★ 5 active flavors of quarks in proton,
- ★ CTEQ, CT10, and MHHT14 sets of PDFs,
- ★ choice for PDFs: $Q = M_{sc} = M$.

We impose the experimental restriction conditions

★ on the detected lepton angle $-\zeta^* \leq \cos \theta \leq \zeta^*$ (or on the rapidity $|y(l)| \leq y(l)^*$); for CMS detector the cut values of ζ^* (or $y(l)^*$) are determined as

$$\zeta^* \approx 0.986614 \quad (\text{or } y(l)^* = 2.5),$$

★ the second standard CMS restriction $p_T(l) \geq 20 \text{ GeV}$,

★ the “bare” setup for muon identification requirements (no smearing, no recombination of muon and photon/gluon).

Notations, invariants, coupling constants

The standard set of **Mandelstam invariants** for the partonic elastic scattering:

$$s = (p_1 + p_2)^2, \quad t = (p_1 - k_1)^2, \quad u = (k_1 - p_2)^2. \quad (2)$$

The propagator for j -boson depends on its mass and width:

$$D^{js} = \frac{1}{s - m_j^2 + im_j\Gamma_j}. \quad (3)$$

Suitable combinations of coupling constants are:

$$\lambda_{f+}^{ij} = v_f^i v_f^j + a_f^i a_f^j, \quad \lambda_{f-}^{ij} = v_f^i a_f^j + a_f^i v_f^j, \quad (4)$$

$$v_f^\gamma = -Q_f, \quad a_f^\gamma = 0, \quad v_f^Z = \frac{I_f^3 - 2s_W^2 Q_f}{2s_W c_W}, \quad a_f^Z = \frac{I_f^3}{2s_W c_W}.$$

Two mechanisms: DY and $\gamma\gamma$ -fusion

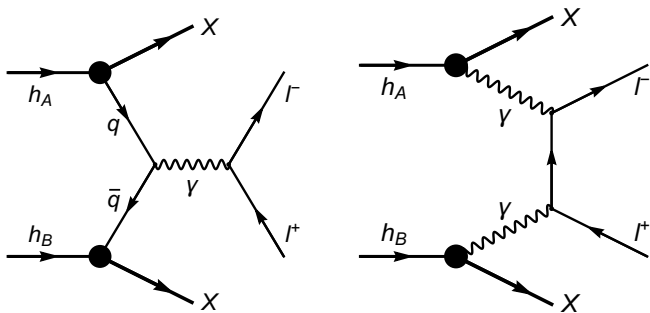


Figure 2: Dilepton production in hadron collisions: left – the Drell–Yan process with virtual photon, right – the photon-photon fusion.

$q\bar{q}$ -annihilation Born: diagrams and cross sections

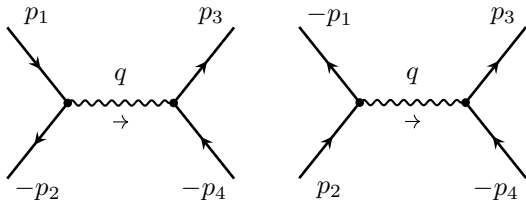


Figure 3: Feynman diagrams of $q\bar{q}, \bar{q}q \rightarrow l^-l^+$ process at Born level.

Parton level:

$$d\sigma_0^{q\bar{q}} = \frac{2\pi\alpha^2}{s^2} \sum_{i,j=\gamma,Z} D^{is} D^{js*} \sum_{\chi=+,-} \lambda_{q\chi}^{i,j} \lambda_{\ell\chi}^{i,j} (t^2 + \chi u^2) dt. \quad (5)$$

$\gamma\gamma$ -fusion Born: diagrams and cross sections

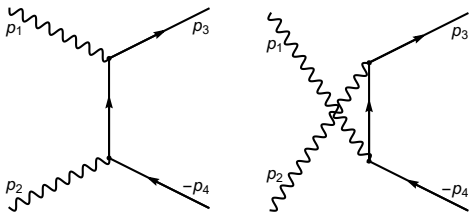


Figure 4: Feynman diagrams of $\gamma\gamma \rightarrow l^-l^+$ process at Born level.

Parton level:

$$d\sigma_0^{\gamma\gamma} = \frac{2\pi\alpha^2}{s^2} \frac{t^2 + u^2}{tu} dt. \quad (6)$$

Hadron level ($\mathcal{C} = \cos\theta$):

$$\frac{d^3\sigma_0^h}{dMdyd\mathcal{C}} = 8\pi\alpha^2 f_\gamma^A(x_1) f_\gamma^B(x_2) \frac{t^2 + u^2}{SM^5(1 - \mathcal{C}^2)} \Theta. \quad (7)$$

DY vs $\gamma\gamma$: diff. cross section $d\sigma/dM$

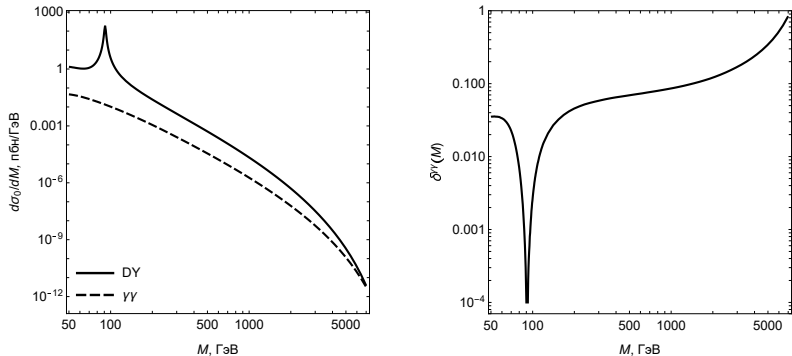


Figure 5: Left – differential Born cross section via M , right – the relative correction $\delta^{\gamma\gamma}(M)$ via M :

$$\delta^{\gamma\gamma}(M) = \frac{d\sigma_0^{\gamma\gamma}/dM}{d\sigma_0^{\text{DY}}/dM}. \quad (8)$$

DY vs $\gamma\gamma$: double diff. cross section $d^2\sigma/dMdy$

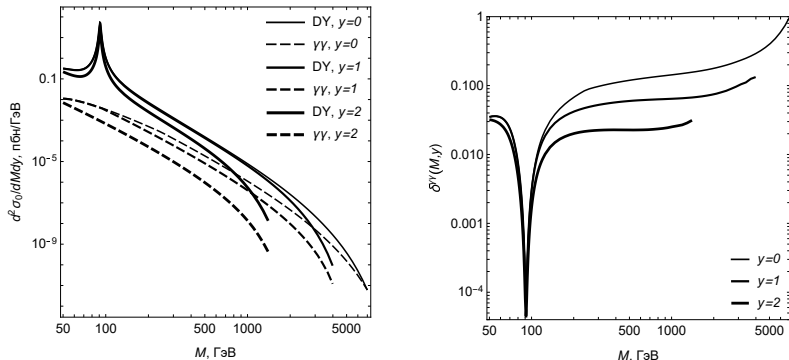


Figure 6: Left – double differential cross sections via M at different y .
right – the relative corrections $\delta^{\gamma\gamma}(M, y)$ via M at different y .

Main features of EWK and QCD RCs calculation

The notations, the Feynman rules and renormalization details are inspired by review of **M. Böhm, H. Spiesberger, and W. Hollik, 1986**:

- ★ **the t'Hooft–Feynman gauge,**
- ★ **on-mass renormalization scheme** ($\alpha, \alpha_s, m_W, m_Z, m_H$ and the fermion masses as independent parameters),
- ★ **ultrarelativistic approximation.**

QCD result can be obtained from QED case by substitution:

$$Q_q^2 \alpha \rightarrow \sum_{a=1}^{N^2-1} t^a t^a \alpha_s = \frac{N^2 - 1}{2N} I \alpha_s \rightarrow \frac{4}{3} \alpha_s, \quad (9)$$

here $2t^a$ – Gell-Man matrices, and $N = 3$.

At the edges of kinematical region (extra large \sqrt{S} , M) the important task is make the RC procedure both accurate and fast. For the latter it is desirable to obtain **the set of compact formulas** for the EWK and QCD RCs.

Leading effect of **Weak RCs** in the region of large M is described by the Sudakov Logarithms (**SL; V. Sudakov, 1956**):

$$\log \frac{m_B^2}{|r|} \quad (B = Z, W; \quad r = s, t, u). \quad (10)$$

Collinear Logarithms (**CL**) play leading role in description of **QED RCs and QCD RCs**:

$$\log \frac{m_f^2}{|r|} \quad (f = e, \mu, q; \quad r = s, t, u). \quad (11)$$

Virtual diagrams: γ and Z

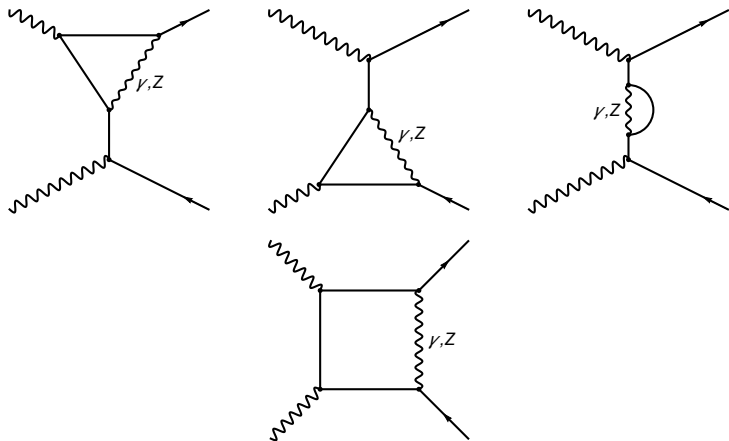


Figure 7: Half of Feynman diagrams set for $\gamma\gamma \rightarrow l^-l^+$ process with additional virtual γ and Z -boson: vertices, electron self energies, boxes. The rest diagrams are obtained by $p_1 \leftrightarrow p_2$.

Virtual diagrams: W

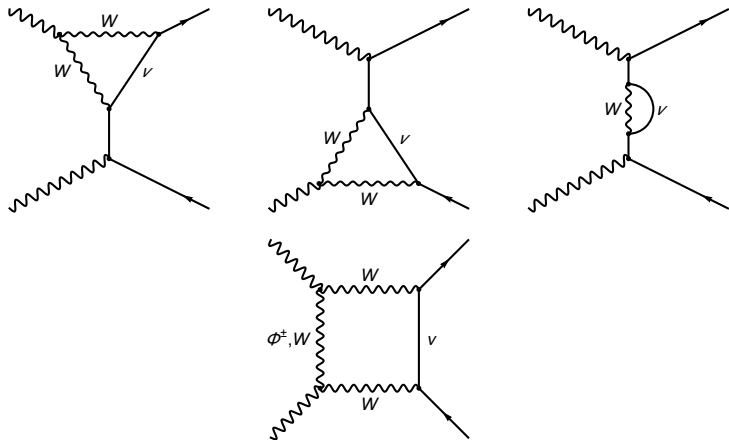


Figure 8: Half of Feynman diagrams set for $\gamma\gamma \rightarrow l^-l^+$ process with additional virtual W -boson: vertices, electron self energies, boxes. The rest diagrams are obtained by $p_1 \leftrightarrow p_2$.

Bremsstrahlung diagrams

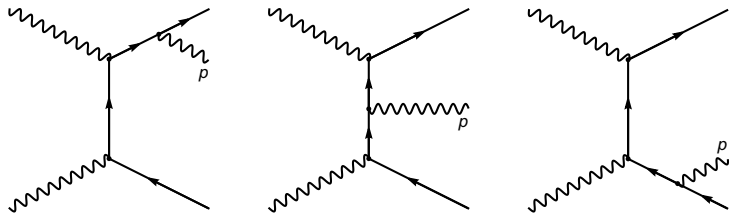


Figure 9: Half of Feynman diagrams set for $\gamma\gamma \rightarrow l^-l^+\gamma$ process. The rest diagrams are obtained by $p_1 \leftrightarrow p_2$.

Virtual + soft contribution

The virtual and soft contributions are factorized before Born cross section (M. Böhm and T. Sack, 1986):

$$\delta_{\text{QED}} = \frac{\alpha}{\pi} \left(\log \frac{4\omega^2}{s} (L - 1) + \frac{\pi^2}{3} - \frac{3}{2} + \frac{tu}{t^2 + u^2} [f(t, u) + f(u, t)] \right),$$

where the function

$$f(t, u) = \frac{s^2 + t^2}{2tu} L_{st}^2 - \frac{3u}{2t} LL_{st} - L_{st}.$$

is entering in the cross section symmetrically (with $t \leftrightarrow u$), and the **collinear** “big” log and angle log look like:

$$L = \log \frac{s}{m^2}, \quad L_{st} = \log \frac{s}{-t}. \quad (12)$$

Weak contributions: Z and W

The **weak corrections** are factorized too:

$$\begin{aligned}\delta_Z &= -\frac{\alpha}{\pi}(v_Z^2 + a_Z^2)\frac{tu}{t^2 + u^2} [G_Z(t, u) + G_Z(u, t)], \\ \delta_W &= -\frac{\alpha}{\pi} \frac{1}{4s_W^2} \frac{tu}{t^2 + u^2} [G_W(t, u) + G_W(u, t)].\end{aligned}$$

Assuming the **HE asymptotic** $\sqrt{s} \gg m_Z$ we get:

$$\begin{aligned}G_Z^{\text{HE}}(t, u) &= \frac{t^3 L_{st}^2}{2u^3} + \frac{tL_{tZ}}{2u}(L_{sZ} + L_{st} - 1) - \frac{tL_{sZ}}{u} - \frac{t^2 L_{st}}{u^2} + \frac{t(27 - 2\pi^2)}{12u}, \\ G_W^{\text{HE}}(t, u) &= \frac{t^2}{su}(\pi^2 - L_{sW}^2) + \frac{t}{u}\left(\frac{\pi^2}{3} + L_{tW}^2\right) - \frac{3u}{2t}L_{tW} - L_{st} + \frac{5u}{4t},\end{aligned}$$

where **Sudakov logs** look like:

$$L_{tB} = \log \frac{-t}{m_B^2}, \quad L_{sB} = \log \frac{s}{m_B^2}; \quad B = Z, W.$$

Independence of unphysical parameter ω

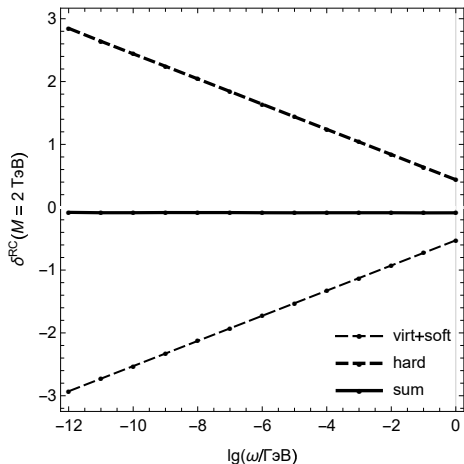


Figure 10: The relative corrections δ^{RC} to differential cross section $\frac{d\sigma}{dM}$ (virtual and soft, hard, their sum) via ω ($M=2 \text{ TeV}$).

Relative correction definition:

$$\delta^{\text{RC}}(M) = \frac{d\sigma_{\text{RC}}^{\gamma\gamma}/dM}{d\sigma_0^{\gamma\gamma}/dM}.$$

ElectoMagnetic corrections to diff. cross section $d\sigma/dM$

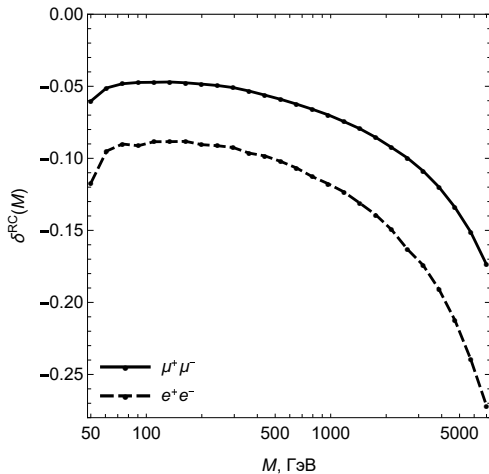


Figure 11: Total relative electromagnetic corrections $\delta^{\text{RC}}(M)$ via M .

ElectoMagnetic corrections to double diff. cross section

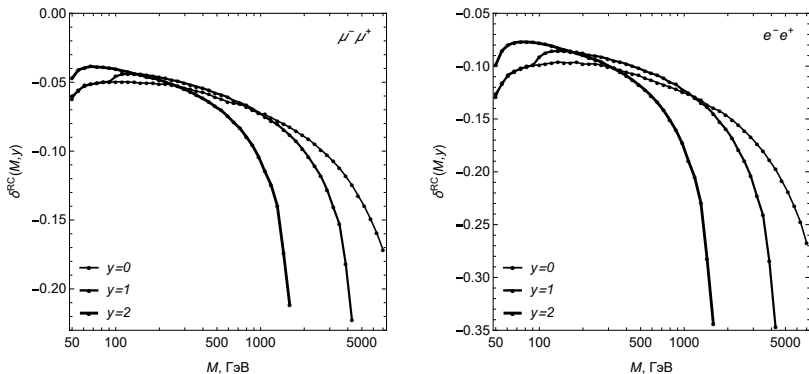


Figure 12: Total relative electromagnetic corrections $\delta^{RC}(M, y)$ to $\frac{d^2\sigma_0}{dMdy}$ via M at different y .

ElectoWeak corrections to $\frac{d\sigma_0}{dM}$ and $\frac{d^2\sigma_0}{dMdy}$

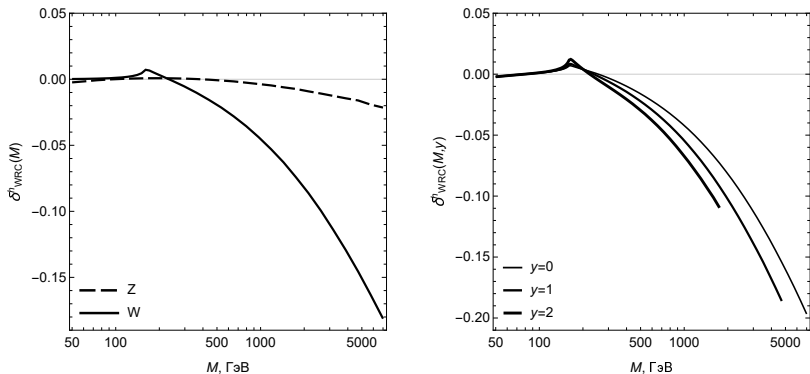
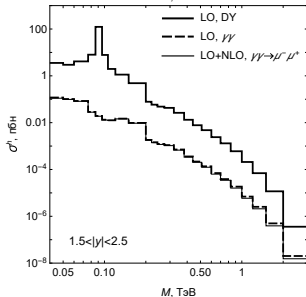
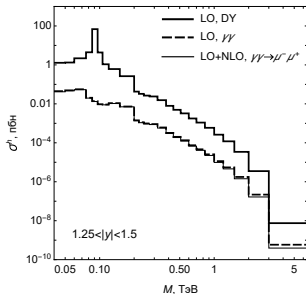
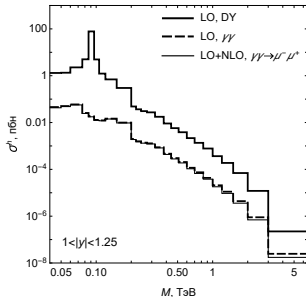
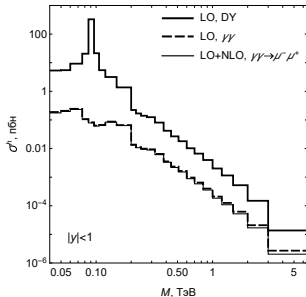


Figure 13: Left (right) – relative electroweak corrections to differential cross section (to double differential cross section at different y) via M .

Total cross sections: standard CMS bins



Forward-backward asymmetry

Forward-backward asymmetry A_{FB} is important observable in dilepton production **with a dual nature – electroweak and kinematical**:

$$A_{\text{FB}} = \frac{\sigma_{\text{F}}^h - \sigma_{\text{B}}^h}{\sigma_{\text{F}}^h + \sigma_{\text{B}}^h}, \quad (13)$$

where according **J. Collins & D. Soper (1977)**:

σ_{F}^h is “forward” cross section ($\cos \theta^* > 0$),

σ_{B}^h is “backward” cross section ($\cos \theta^* < 0$).

In the Collins–Soper system $\cos \theta^*$ looks like:

$$\cos \theta^* = \text{sgn}[x_2(t + u_1) - x_1(t_1 + u)] \frac{tt_1 - uu_1}{M\sqrt{s(u + t_1)(u_1 + t)}}.$$

Forward, Backward (and Experimental) borders

For the case of nonradiative kinematics the $\cos\theta^*$ has especially simple view:

$$\cos\theta^* = \text{sgn}[x_1 - x_2] \frac{u - t}{s} = \text{sgn}[e^y - e^{-y}] \frac{(1 + C)e^{-y} - (1 - C)e^y}{(1 + C)e^{-y} + (1 - C)e^y}.$$

Solving $\cos\theta^* = 0$ we get **two conditions** for border dividing the regions of σ_F^h and σ_B^h :

$$y = 0, \quad C \equiv \cos\theta = \text{th } y.$$

The CMS experimental condition $|\cos\theta| < \zeta^*$ is trivial but the second one $|\cos\alpha| < \zeta^*$ is rather sophisticated:

$$\cos\left(\arccos \frac{\cos\theta - \text{th } y}{r} + \arcsin \frac{\sin\theta \text{th } y}{r}\right) = \pm\zeta^*,$$

where

$$r = \sqrt{1 - 2\cos\theta \text{th } y + \text{th}^2 y}.$$

Forward, Backward (and Experimental) regions

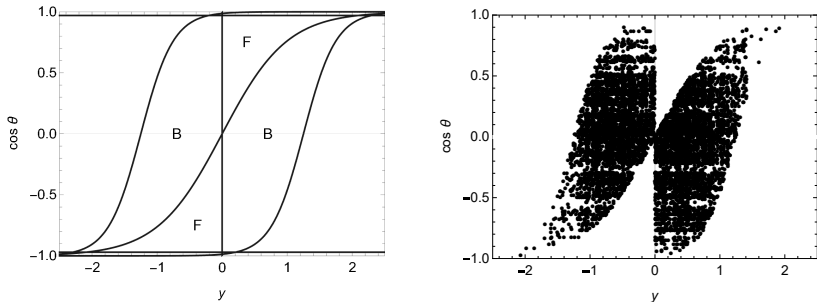


Figure 15: Left – Forward, Backward and CMS regions in y and $\cos \theta$ variables (**borders are:** $y = 0$, $\cos \theta = \text{th} y$, $\cos \theta = \pm \zeta^*$, and $\cos \alpha = \pm \zeta^*$, where $\zeta^* \approx 0.9866$), right – the points sampled by Monte-Carlo generator of VEGAS for **Backward CMS region**.

Interplay of DY and $\gamma\gamma$ for A_{FB} : numerical effect

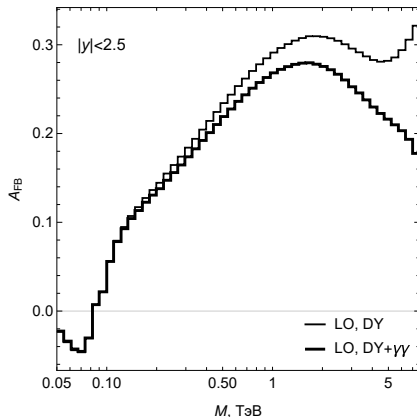


Figure 16: The Born forward-backward asymmetry via M at CMS LHC setup: for **Drell–Yan mechanism** – thin line, for **both mechanisms** (DY and $\gamma\gamma$ -fusion) – thick line.

Interplay of DY and $\gamma\gamma$ for A_{FB} : explanation

As the Born process $\gamma\gamma$ -fusion has **pure electromagnetic nature**, then

$$A_{\text{FB}}^{\gamma\gamma} = 0.$$

Therefore the F- and B- cross sections are equal:

$$\sigma_{\text{F}}^{\gamma\gamma} = \sigma_{\text{B}}^{\gamma\gamma} = \Delta.$$

The $\gamma\gamma$ -fusion cross section has the scale comparable with DY one **at large M region**. Expanding the net asymmetry (DY+ $\gamma\gamma$) in series on Δ we get:

$$A_{\text{FB}}^{\text{DY}+\gamma\gamma} \approx A_{\text{FB}}^{\text{DY}} \left(1 - \frac{2\Delta}{\sigma_{\text{F+B}}^{\text{DY}}} \right).$$

This effect (the decreasing of net asymmetry at large M) is well seen in Fig. 16 starting with $M \sim 300$ GeV.

A_{FB} for Run3 of CMS LHC: $\mu^+\mu^-$, DY

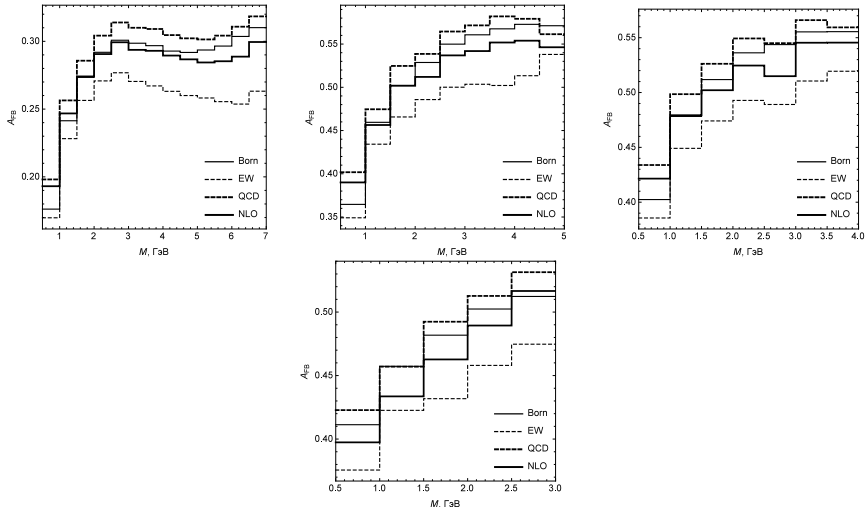


Figure 17: A_{FB} for $\mu^+\mu^-$ -production: top – $|y| < 1$ and $1 < |y| < 1.25$, bottom – $-1.25 < |y| < 1.5$ and $1.5 < |y| < 2.5$.

A_{FB} for Run3 of CMS LHC: e^+e^- , DY

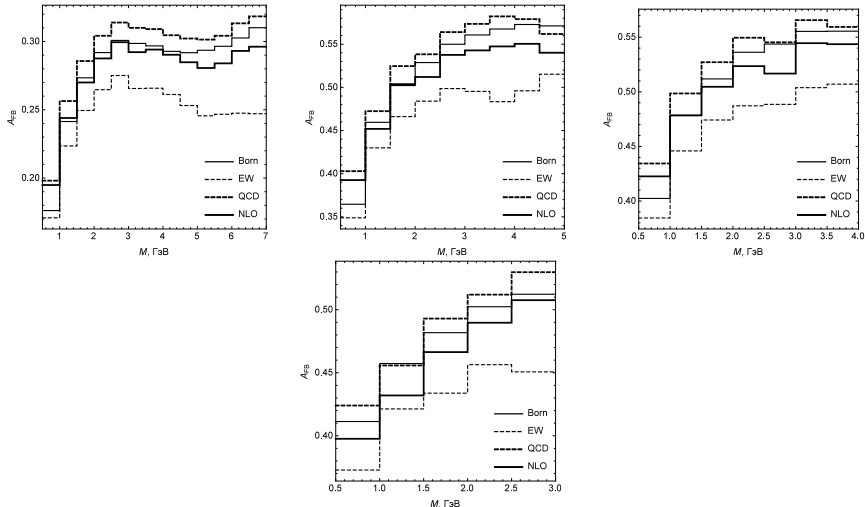


Figure 18: A_{FB} for e^+e^- -production: top – $|y| < 1$ and $1 < |y| < 1.25$, bottom – $-1.25 < |y| < 1.5$ and $1.5 < |y| < 2.5$.

A_{FB} for Run3 of CMS LHC: $\mu^+\mu^-$, DY and $\gamma\gamma$

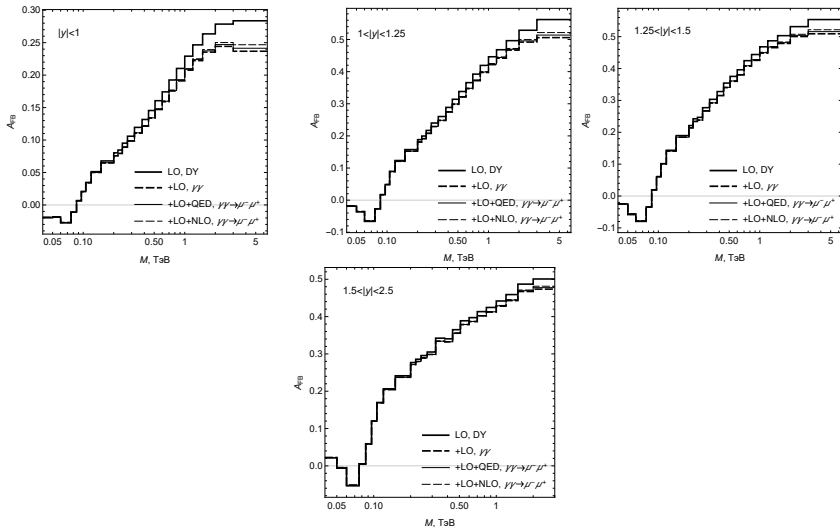


Figure 19: Forward-backward asymmetry A_{FB} for $\mu^+\mu^-$ -production.

Corrected forward-backward asymmetry is defined as follows

$$\begin{aligned} A_{\text{FB}}^c &= \frac{\sigma_{\text{F}}^0 + \sum_c \sigma_{\text{F}}^c - \sigma_{\text{B}}^0 - \sum_c \sigma_{\text{B}}^c}{\sigma_{\text{F}}^0 + \sum_c \sigma_{\text{F}}^c + \sigma_{\text{B}}^0 + \sum_c \sigma_{\text{B}}^c} = \\ &= \frac{\sigma_{\text{F}}^0 - \sigma_{\text{B}}^0}{\sigma_{\text{F}}^0 + \sigma_{\text{B}}^0} \times \frac{1 + \sum_c \delta_-^c}{1 + \sum_c \delta_+^c} = \\ &= A_{\text{FB}}^0 \times \frac{1 + \sum_c \delta_-^c}{1 + \sum_c \delta_+^c}, \end{aligned} \tag{14}$$

where

$$\delta_-^c = \frac{\sigma_{\text{F}}^c - \sigma_{\text{B}}^c}{\sigma_{\text{F}}^0 - \sigma_{\text{B}}^0}, \quad \delta_+^c = \frac{\sigma_{\text{F}}^c + \sigma_{\text{B}}^c}{\sigma_{\text{F}}^0 + \sigma_{\text{B}}^0}.$$

Dependance of relative corrections on M

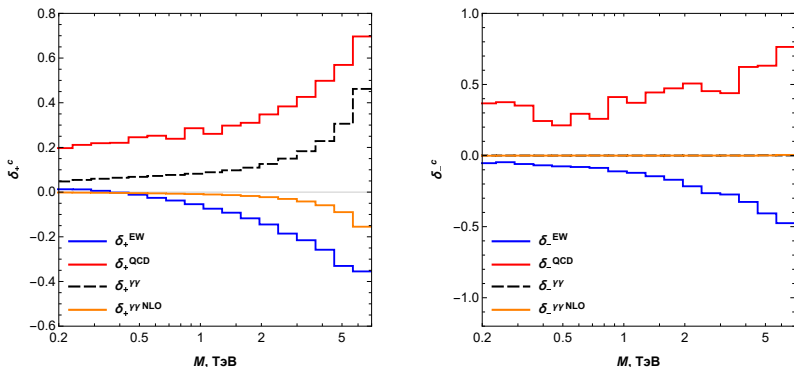


Figure 20: Additive relative corrections: left – “plus”, right – “minus”.

Example (for the last bin, $M/\text{TeV} \in [5.66, 7]$):

$$A_{\text{FB}}^c = A_{\text{FB}}^0 \times \frac{1 - 0.475 + 0.764 + 0.001 + 0.005}{1 - 0.355 + 0.697 + 0.462 - 0.155} = A_{\text{FB}}^0 \times 0.785.$$

One more mechanism: inverse γ emission

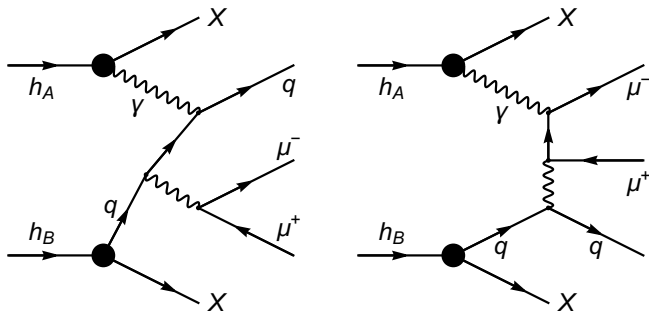


Figure 21: Dilepton production in hadron collisions: left – inverse γ emission with quark, right – inverse γ emission with muon.

Conclusions & Acknowledgement

- ★ **The NLO EWK** corrections to dilepton production with Drell–Yan and $\gamma\gamma$ -fusion mechanisms have been studied.
- ★ It has been ascertained that the considered in Run 3 region radiative corrections change the cross sections and A_{FB} **significantly**.
- ★ I would like to thank the **RDMS CMS group** members for the stimulating discussions and **CERN (CMS Group)** for warm hospitality during my visits.
- ★ This work was supported by the **Convergence-2025** Research Program of Republic of Belarus (Microscopic World and Universe Subprogram).
- ★ The numerical calculation was performed partially by “**HybriLIT**” Heterogeneous Platform of the Laboratory of Information Technologies of JINR.